

Borehole Inner Surface Visualization System with Vibration Cancellation and Trajectory Smoothing Based on Optical Monocular Video Camera

Nan Zong¹ ^a, Waleed Al-Nuaimy¹ ^b, Heba Lakany¹ ^c and Paul Worthington²

¹*School of Electrical Engineering, Electronics and Computer Science, University of Liverpool, Brownlow Hill, Liverpool, U.K.*

²*Department of Engineering & Development, Robertson Geologging Ltd., York Road, Deganwy, U.K.*

Keywords: Geological Data Logging, Monocular Video, Image Processing, Data Visualization.

Abstract: The rapid digitization and modelling of the planet brings with it increased demand for the tools necessary to process and visualize disparate streams of multivariate and often highly complex geophysical data streams. The rationalization of detection hardware and the integration of sensors offers the potential to economically visually explore and map geophysical environments such as the interior of subterranean boreholes. This paper addresses the challenge of visual reconstruction of the geometry of the inner surface of a borehole from video data collected via a monocular optical camera. We introduce a novel system of algorithms to unwrap the cylindrical borehole inner surface data and to compensate for the offsets and errors arising during data acquisition. Three modules are designed for this task: Unwrapping module consisting of algorithms to generate visualization results of borehole inner surfaces; Vibration cancellation module that compensates for rotation and drift errors caused by the movement of detectors, balancing computational cost and performance; Trajectory smoothing based on image convolution signal processing methods to filter out anomalies and interruptions that arise as a result of the other processing stages. The proposed system integrates these modules to generate planar side-view images with a high level of spatial accuracy. This system also contributes to establish a novel and easy-to-access visualization tool of boreholes with simplified detectors that only consists of a monocular camera and a fixed circular LED band. Results have demonstrated the system is capable of resisting high frequency drift and the effects of rotation and vibrations in harsh subterranean environments. This novel combination of video and image processing marks a significant improvement over currently available or published borehole video exploration techniques, and can be further extended and enhanced to deliver more accurate multi-sensor 3D modeling and reconstruction of the complex inner structure of geophysical boreholes.

1 INTRODUCTION

As the geologic exploitation of the planet is becoming increasingly important for understanding the world around us, the academic domains of geophysics and geology are attracting growing attention from researchers attempting to further facilitate the digitisation and visualisation of this exploration process.

Most researchers are focusing on providing more precise measurements of dimensions following the trend of the evolution of more advanced sensing hardware, for example, data fusion of exploitation sensors such as sonar and LIDAR (Thiele et al., 2021; Pohl and Genderen, 1998). However, when it comes

to the exploration in a harsh environment, systems with complex and fragile sensors are facing challenges of robustness problem where delicate sensors must be strictly protected against high-pressure, high-temperature, and underwater conditions (Thiele et al., 2021; Pohl and Genderen, 1998). Thus, this trend is being questioned since the system complexity will be greatly aggravated of which the efficiency and cost are not balanced. What is worse, due to the limitation of commercial cost, the spatial constraints and reliability demand against complicated designs, detectors can often be constructed with limited sensors only.

Due to the constraints of the operating conditions, it is normally considered that enhancing the strength or sealing technology should be applied to the detectors. But making detectors larger and even more complex as other researches usually do could be accompa-

^a  <https://orcid.org/0009-0007-1261-3671>

^b  <https://orcid.org/0000-0001-8927-2368>

^c  <https://orcid.org/0000-0003-3079-0392>

nied by a remarkable increment of manufacturing and processing cost. Instead of enlarging the system, our research starts to focus on the simplification of system without losing much performance of the data recording function of borehole inspection by migrating difficulties of hardware layer to software post processing layer.

In this paper, based on the monocular tele-viewer provided by the cooperator company, our contribution is the proposition of a system design that integrates all related solutions to handle image re-projection, vibration cancellation and trajectory smoothing of a borehole side view visualizer. The "Side-view Unwrap Module" we designed introduces methods of sampling with modifiable parameters of unwrapped resolution need to be provided in order to generate clear and exquisite visual results. The algorithms involve in pixel sampling and extraction, and are designed based on polar coordinates, prefixing the center of borehole as origin. This offers to sample valid pixels on a ring of borehole inner surface with higher resolution after interpolations. Settings of sampling resolution and range are configurable to adapt to different borehole logging files and conditions.

After obtaining the unwrapping results, it is considered that the performance is largely influenced by camera direction change and position drifting, which can be concluded as vibrations. Thus in the second design of "Vibration Compensation Module", methods are developed, aiming to stabilise the visual results collected by the optical camera. Vibrations under the described usage scenario are considered to be rotation errors and drifting errors compared to the center of boreholes as origins. A mixed algorithm design of cylindrical borehole center finder and rotation compensation with cross-correlation is proposed, which has good balance in time cost and performance compared to other video stabilizers when compensating drifting and rotation errors, and particularly effective at smoothing high frequency vibrations.

To improve the defaults of compensated results (interruptions between rows might occur after vibration cancellation), a "Trajectory Smoothing Module" based on convolution of a preset window size is deployed. This smooths the interruptions of pixel shifts on unwrapped image which occur during compensation and unwrapping procedure. This helps to improve the consistency of visual inspection of boreholes.

The final results processed after the entire procedure prove that this visualizing system can not only effectively extract clear side-view images of boreholes, but also can resist high frequency vibrations and provide continuous visual results with good balance between

processing time cost and performance.

2 RELATED WORKS

2.1 Problems and Challenges

In this part, a large number of problems and challenges occur in the field of logging borehole data and visualization are widely discussed. Three main problems occurs during the construction of borehole visualization system with monocular camera and fixed illumination LED Ring:

- Pixels Extraction and Image Re-projection in Unwrapping Procedure;
- Compensation of Vibration Brought by Movement of Detector;
- Trajectory Smoothing and Visualization Improvement of Inspection Results.

First of all, visual data collection problem is raised, involving video clarity, geological feature extraction and data quality assessment. Such problems become especially evident when the detectors are always deployed under extreme situations - liquid medium with impurities, temperature change and dark illumination conditions. This limits the selection of reliability of sensors, and the complexity of detectors is required to be as simple as possible to avoid potential damage. Thus, how to obtain good visual results from simple sensors, how to enhance the captured visual data and how to filter disturbances are urgent and charming challenges that need to be conquered in order to unwrap and render a high quality inner surface texture of boreholes before presenting the visual results of boreholes geological log data.

2.2 Background Research

2.2.1 Pixel Extraction and Video Re-Projection

Many researchers worked on unfolding and mapping video frames from projection on spherical canvas (which is the nature physics of monocular cameras) to cylindrical or even flat canvas, with distortion correction and effective interpolation. There are two types of distortion involved in the first phase of re-projection: Radial distortion and tangential distortion, which are brought by the physical constraints of sensors with semi-spherical lens. To cancel radial distortion, (Hartley and Kang, 2007) proposed effective methods that determines the radial distortion and also computes the center of radial distortion

in a parameter-free way, not relying on any particular radial distortion model. For tangential distortion cancellation, proposals of (Beauchemin and Bajcsy, 2001) models the lens radial and tangential distortions and determines the optical center and the angular deviations of the CCD sensor array within a unified numerical procedure.

After fixing distortion and determining inner parameters of the camera, re-projection methods can be applied. A planar coordinates to polar coordinates transform is implemented to sample pixels in a circular order, with radius and angle step for each sample selected as parameters. This allows to extract points from a downwards (upwards) view of image to the projection points on side view as a cylindrical surface is usually considered as borehole inner surfaces. This kind of re-projection distinguished itself from normal demand of image projections due to the special use case of cylindrical borehole geometry.

2.2.2 Vibration Compensation

In the aspect of vibration and error correction of moving cameras, stabilisation methods are also widely taken into consideration with various methods proposed.

In traditional image processing perspective, video vibration cancellation involves in multi sensor data fusion. A previous research of this work includes a camera position correction method using acoustic sensor. By calculating the amplitude and travel time of the ultra-sonic wave, it is possible to find out the relative displacement of the detector (Al-Sit et al., 2015). Taking another example of OIS (Optical Image Stabilization), by using the data from gyro sensors, the camera's movement and vibration can be compensated by the three dimensional angular acceleration of the device (Cardani, 2006). Some researchers have also started to focus on mechanical stabilizers controlled by magnetic field which can be adjusted using electric currents, with tracks that can move the camera on the same plane, even though the angular oscillation and rotation error cannot be compensated (Bereska et al., 2013). The most state-of-art vibration cancellation now includes OIS, mechanical stabilizer and gimbal stands. Gimbal stands use multi-motors to provide three dimensional movement for cameras to compensate against sudden unexpected movement (Rajesh and Kavitha, 2015).

For digital video stabilizer without the use of specific hardware, several newly proposed researches are listed (Souza and Pedrini, 2019). The 2D digital video stabilization process is usually implemented in three steps: (i) camera motion estimation, (ii) removal of unwanted motion and (iii) generation of the

corrected frames, which applies affine transforms to align the video frames according to the remaining motion. As a widely welcomed research direction, Monocular V-SLAM (Visual Simultaneous Localizing and Mapping) issues are also considered an effective way to estimate camera pose and stabilise, not only in Geophysics but also in fields as Autonomous Driving and Robotic Perception. ORB-SLAM2 proposed a very effective way to solve camera location and pose with epipolar geometry and ORB key feature points extraction (Mur-Artal and Tardós, 2017). Other V-SLAM algorithms also outperforms in certain criteria but they mainly share similar performances in general.

2.2.3 Trajectory Smoothing

Trajectory smoothing is considered as a post processing phase after obtaining compensated results from vibration cancellation phase. Similar to Monocular V-SLAM methods, trajectory smoothing also use key points extraction and tracking in frame sequences to regenerate camera pose and location. Then sliding windows of smoothing range is defined to cancel high frequency vibrations, which might not be effectively stabilised in the vibration cancellation phase (Souza and Pedrini, 2018). Here we studied two classic trajectory smoothing algorithms: (i) Moving average, which calculates the average in a range of neighbors as the value of the center point (ii) Savitzky-Golay Filter, a filtering method based on local polynomial least squares simulation (Press and Teukolsky, 1990).

Both methods are considered foundation and cornerstone of points trajectory smoothing methods which guarantee good enough performances in camera stabilisation. Meanwhile, trajectory smoothing can not only filter high frequency vibrations, but also can interpolate trajectory way point if an interruption (or a large dislocation in neighboring frames of a sequence) occurred in the results of vibration cancellation.

3 SYSTEM DESIGN & PRINCIPLE

Our system is designed to accomplish a pipeline procedure of processing. Expected input data are no more than 2D color images that is listed in a continuous time sequence. The content of these frames are view ports that look downwards to the bottom of boreholes, captured by a monocular camera. A fixed illumination source using a LED ring with a max intensity measured at 12lm per LED diode is integrated

around the camera, and the detector supports automatic brightness adjustment and white balance. Also, a mechanical centraliser is attached to maintain the position and direction of the detector to the center of the borehole, facing downwards the center of the bottom. These mechanical and designs facilitate the pre-processing of the recorded images thanks to a relatively good quality of recorded video1.



Figure 1: Detector provided by sponsor company.

Three modules are designed to handle each tasks, described as follows.

3.1 Side-View Unwrapping and Re-Projection

A "Side-view Unwrapping Module", aiming to deal with pre-processing and re-projection of image data captured. The work flow of this module first involves in cancellation of the distortion by recalculating the inner parameter of the camera, followed by steps of remapping pixels in the shape of a sampling ring to a unwrapped side-view. This sampling and remapping is based on the assumption of cylindrical boreholes drilled artificially. For the distortion cancellation, the calibration of inner parameter focuses on the radial distortion and tangential distortion cancellation. These two distortions are modelled as below: For radial distortion: For tangential distortion: Solutions to remap the image using the matrix of distortion are given as follows: Thanks to (Hartley and Kang, 2007) and (Beauchemin and Bajcsy, 2001), the inner parameters of the camera are effectively calculated using the corresponding calibration tools in OpenCV library.

After having corrected the camera, a mapping relational expression from pixels on the sampling ring using polar coordinates to the rectangular plane coordinates of pixel on the unwrapped plane is established:

$$P(\rho, \gamma) = \begin{cases} P_x(\rho, \gamma), \\ P_y(\rho, \gamma), \end{cases}$$

where

$$P_x(\rho, \gamma) = \rho \cos(\gamma),$$

$$P_y(\rho, \gamma) = \rho \sin(\gamma),$$

This allows the visualizer to analyse and remap the semi-spherical space capture by the camera towards the bottom of boreholes to the cylindrical side-view around the detector. These flattened images are defined as the unwrapped image results of the inner surface of boreholes.

3.2 Vibration Cancellation

Regarding the method applied and unwrapped image results obtained in the first module, a noticeable imperfectness occur that sudden shifts of pixels, or "interrupts" greatly influenced the continuity of appearance of visualization. These interrupts are caused by sudden vibrations of the camera. These vibrations can be decomposed and modelled as two types: translation movement on the plane of the camera lens and rotation with the axis in the direction of the length of the detector. Therefore, a second Module named "Vibration Compensation Module" is implemented aiming to cancel these two types of vibration error. For cancelling the translation movement error, a borehole center finder is applied to fix the captured image center to the borehole center.

The according algorithm uses the dark part of the borehole image as the center part of the borehole which might contain the borehole center. A ellipse finder is used to find out the largest ellipse matched to the contour of the dark area in the borehole video frames. This potentially returns the center of the borehole that is also considered as the relative loaction of the camera:

This coordinates also indicate the relative location of the detector/camera comparing to the borehole.

To diminish the rotation type of error, cross-correlation method is used to detect the rotated number of pixel in the unwrapped image. Cross-correlation is first used to compare the similarity or pattern between two time-oriented signals, and it can also yield the delay of time which can make a maximum match of pattern of two signals. Using this property, it is possible to measure the rotation error (considered as the delay of time in time-oriented signals) of two rows of pixels. In order to implement, the two pixel rows to compare should firstly be normalized. In our case, in a 8 bit image, the normalization is in the range of [0, 255]. The time axis is replaced by the index of pixels in the row, and the index corresponds to the sampling angle of each frame as a results of the first module. Then, cross-correlation is calculated

Algorithm 1: Borehole Cylindrical Center Finder.

Input: input video V
Output: output center location $C_{borehole}$

- 1: Using OpenCV ellipse matching to find the center of borehole
- 2: Load video V and get video resolution R
- 3: Get current frame F
- 4: Set center of resolution $C_{image} = 0.5 \times (R)$
- 5: Set $C_{temp} = C_{image}$
- 6: **if** F in frames sequence of V **then**
- 7: $G = GaussianBlur(F)$
- 8: $Gr = ColorConvertGrey(G)$
- 9: $B = Binarization(Gr)$
- 10: **if** found $Contours$ in B **then**
- 11: **for** Ctr in $Contours$ **do**
- 12: $Ctr = Largest(Contours)$
- 13: **if** Ctr area in $AreaRange$ **then**
- 14: $E = Matchellipse(Ctr)$
- 15: $C_{contour} = ellipseCenter(E)$
- 16: **if** $distance(C_{contour}, C_{image})$ in $DistanceRange$ **then**
- 17: $C_{borehole} = C_{contour}$
- 18: $C_{temp} = C_{contour}$
- 19: **else**
- 20: $Ctr = NextLargest(Contours)$
- 21: **else**
- 22: $C_{borehole} = C_{temp}$
- 23: $F = NextFrame$
- return** $C_{borehole}$

between two neighboring rows to compare their similarity.

This algorithm utilizes the principle that if a rotation movement of camera occurs, two continuous rows extracted will not be similar anymore without rotation compensation, with similarity and according shifted pixels are given by the value of cross-correlation and corresponding delay. Thus, if the module can find the the maximum value and the according delay of index, they can be used to compensate thee rotation. If the maximum value of cross-correlation remains at a low level (lower than a threshold), the module can filter two neighboring rows that have a huge difference of appearance that breaks the visual continuity. Therefore, these two rows are proven to be unsuitable for compensation in this case.

3.3 Trajectory Smoothing

After the first two modules, in order to avoid sudden interrupts that are not suitable to be compensated as described previously, the module "Trajectory Smoothing Module" is finally deployed to ameliorate the experience of visualisation for users. For

Algorithm 2: Rotation Compensation Using Cross Correlation.

Input: input a row of unwrapped pixels $R1$
Output: output similarity S and rotated number of pixels $R_{rotated}$

Using Cross Correlation to Evaluate Similarity & Rotation

- 2: $R2 = NextRow(R1)$
- $S_{list} = CrossCorrelation(R1, R2)$
- 4: **while** $R2$ is not $None$ **do**
- $S_{max} = max(S_{list})$
- 6: **if** $S_{max} \geq SimilarityThreshold$ **then**
- $S = S_{max}$
- $R_{rotated} = indexof(S)$ in S_{list}
- else**
- 10: Cannot Compensate
- Pass
- 12: $R1 = R2$
- $R2 = NextRow(R1)$
- return** $S, R_{rotated}$

artificially exploited boreholes, inner surfaces are always continuous in textures and patterns. When an irreparable structure or movement of camera is encountered, in order to solve the discontinuity that should not occur, trajectory smoothing algorithm is introduced.

Two types of interruption of continuity of camera trajectory according to the vibration cancellation module are considered: Drifting interrupt caused by drifting and rotary of camera. By analysing the expected results of vibration cancellation module, the trajectory anomalies are mainly outlier noises that can be effectively filtered by using a local polynomial least squares simulation based Savitzky-Golay Filter(S-G filter). This filter performs in a fast speed with good performance of calculating average in an interval, and keeps the data unmodified at both borders (the beginning and ending sections) of the trajectory. It can also maintain the shape of signals while filtering outliers and smoothing sharp turning points in a sliding window using polynomial fittings. The S-G filter is applied once when the pixel rows (results of module 2) are accumulated to a number of the window size which can effectively lower the consumption of calculation resources.

For a filtering window size of $n = 2m + 1$, signal values to be filtered as $x = (-m, -m + 1, \dots, 0, 1, \dots, m - 1, m)$, and a polynomial degree of $k - l$ used to fit, the fitted value of the window y is:

$$y = a_0 + a_1x + a_2x^2 + \dots + a_{k-1}x^{k-1}$$

Thus, a system of linear equations with k elements can be constructed. In the form of matrix:

$$Y_{(2m+1) \times 1} = X_{(2m+1) \times k} \cdot A_{k \times 1} + B_{(2m+1) \times 1}$$

Here, Y is the matrix of fitted values and X is the input signal. Thus, the coefficients of the polynomial A and the predicted values of Y can be solved:

$$\hat{A} = (X^T \cdot X)^{-1} \cdot X^T \cdot Y$$

$$\hat{Y} = X \cdot A = X \cdot (X^T \cdot X)^{-1} \cdot X^T \cdot Y = E \cdot Y$$

with:

$$E = X \cdot (X^T \cdot X)^{-1} \cdot X^T \cdot Y$$

4 EXPERIMENTS & RESULTS

Since this research work is based on borehole inspection, a borehole detection hardware tool is applied as a platform for following researches. A visualization tool and according hardware detector are shown in Figure 2.

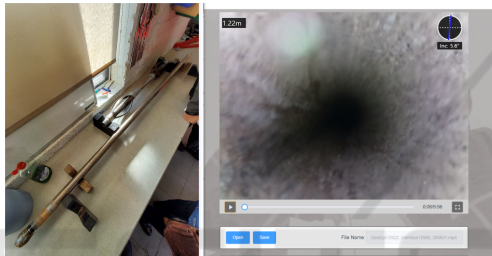


Figure 2: Detector and video player provided by sponsor.

Data used in this section are collected using the mentioned borehole detector above, in different inspection environment of boreholes, provided by partner company. For example, a drilled test borehole located in Deganwy, Wales, United Kingdom. Data are logged as video files encoded by h264 format in mp4 container.

The according field of view (FoV) of this video is measured at 45 degrees both horizontally and vertically after cropping. The resolution cropped is 800*600. The detector itself has a mechanical centralizer that can relatively stable the camera at the center of the borehole.

The workflow of the data recording is that the detector fixed on one end of the winch rope is lowered down into the borehole facing towards the bottom. The moving speed is kept as uniform and as slow as possible to generate stable and clear videos of the inner surface shown in Figure 3.

4.1 Side-View Unwrapping

The function of this module is to find out suitable positions of pixels which are used in the unwrapping.

First of all, the inner parameter of the camera is tuned by 8 checker board images from standard



Figure 3: Winch used to send detector down into the test borehole.

OpenCV documents with 22cm as the width of each square pattern.

The generated K and D matrix are as follows, where K matrix represents the intrinsics of the camera, or the focus and center of camera image, and D matrix recalculates the tangential/radial distortion coefficients of the camera.

$$K = \begin{bmatrix} f_x & 0 & c_x \\ 0 & f_y & c_y \\ 0 & 0 & 1 \end{bmatrix}$$

$$D = [k_1 \quad k_2 \quad p_1 \quad p_2 \quad p_3]$$

where

- f_x, f_y , the focuses on x axis and y axis of the camera
- c_x, c_y , the center pixel location of the camera image
- k_1, k_2, p_1, p_2, k_3 , the radial/tangential distortion parameter

Here is an example figure (Figure 4) that presents results before and after anti-distortion using the detector and according intrinsic matrix and distortion matrix K, D .

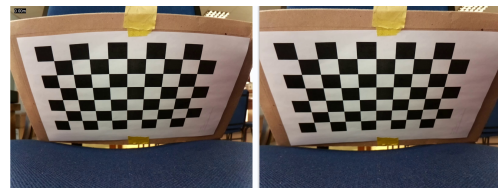


Figure 4: Before and after distortion compensation.

The borehole shape is cylinder-like, thus a "Scan Circle" is selected to fix the positions of pixels, which corresponds to one extracted row in the unwrapped image.

Polar coordinates are used, with origin point chosen at the center of the borehole. Here, $P(\rho, \gamma)$ represents the rectangular planar coordinates for a pixel at location (P_x, P_y) on the video frame captured in the

polar coordinates. i is the index of the sampled pixel on the unwrapped row. Two parameters are designed to control the selections of pixels on the "Scan Circle" with index i :

$$P(\rho, \gamma)[i] = \begin{cases} P_x(\rho, \gamma)[i], \\ P_y(\rho, \gamma)[i], \end{cases}$$

where

$$P_x(\rho, \gamma)[i] = \rho \cos(i \times \gamma),$$

$$P_y(\rho, \gamma)[i] = \rho \sin(i \times \gamma),$$

- ρ , the pixel distance between the center and the pixel
- γ , the angle sampled with a certain step
- i , the index of the sampled pixel in anti-clockwise order

It is noteworthy that the ρ value should be limited according to camera profile. Due to the focus of camera is at around 3mm, the detection range of clear image will be at a pixel distance interval from 60 to 240 pixels. As the resolution of video clip is fixed at 800*600, for each "Scan Circle" with radius from 60 pixels to 240 pixels, the resolution of minimum number of pixels are from 180 to 720.

As a result, in this proposed unwrapping method, the rho value of 240 and the γ step value of 0.5 degree are selected to generate good quality side view pixels with 720 pixels chosen per row in the unwrapped image.



Figure 5: Original frame and corresponding unwrapped side view image.

Here is a chosen frame from the video and its corresponding unwrapped row (to visualize better, several rows are displayed together as a band of image block in Figure 5).

The results showed good quality of unwrapping when the camera stays relatively stable at the center of the borehole. However, when the detector touches the wall of the borehole, vibrations and rotations are inevitable, which might cause the non-continuity of unwrapped rows from continuous frames. This triggers the functionality of next module, improving the performance of this unwrapping method by providing compensation of camera centralization and rotation.

4.2 Vibration Compensation

In this section, an experiment corresponding to the system design of combining cross correlation and ellipse center finder is implemented to deal with centralisation and rotation cancellation tasks. Since the center of the video (of a borehole) is always a dark ellipse due to the poor brightness illumination of the bottom of boreholes, it is easy to extract an ellipse shaped center and the sampling "Scan Circle" can be re-configured to compensate the drifting of camera caused by outer influences. The center of these ellipses can represent the trajectory of the camera moving downwards to the bottom of the borehole in Figure 6.

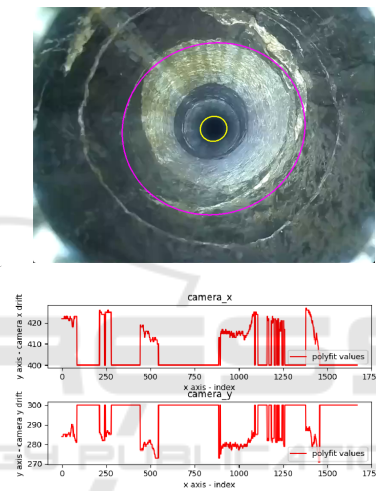


Figure 6: Ellipse center (yellow) and camera trajectory.

In terms of rotation compensation, the extracted row of pixels are considered as a 1 dimensional signal. By comparing continuous rows of pixels, it is possible to find out if pixels are rotated according to the differences between them. Because of the continuity of pixels rows, the similarity of these signals should remain at a high level. Thus, cross correlation of two neighboring signals can provide solutions of how many pixels are drifted before and after by calculating the maximum cross correlation value and according delay applied to following rows. Here, we take two continuous rows as an example of cross-correlation rotation correction⁷. Each row includes 720 pixels according to the sampling gamma of 0.5 degrees in the test of previous unwrapping module.

Since the calculation of cross-correlation considers a full range number of pixels in one row from index 0 to 719, these samples are therefore repeated and reconstructed as a signal of tow periods (index from 0 to 1439) of the original input. As a result, the

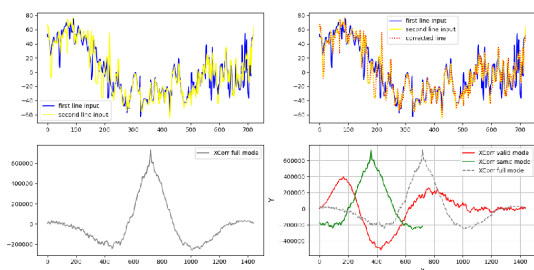


Figure 7: Rotation compensation before and after.

cross-correlation value reaches the maximum point at a pixel shifting (or "delay" of signal) number of 730 pixels. This indicates that the input row should be rotated with a delay of pixels of 11 pixels to make the two rows match each other to maximum. The maximum similarity in this case reaches more than 65000 (signals normalized from 0 to 255). This proves that if a rotation compensation of 11 pixels anti-clockwise is applied to the next row, the rotation error between these two neighboring rows can be effectively diminished.

Below are the visualized results when the center finder and rotation compensation module tested on the entire video. It can be seen that the original unwrapped data on the left is intensively distorted in the red block area. This reflects to a sudden collision of the camera and the wall in the logged video. On the right, the compensated results successfully corrected this collision that caused drifting and rotation of the detector, which can be obviously seen in Figure 8.

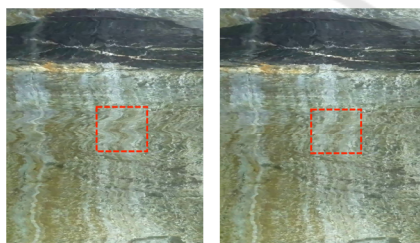


Figure 8: Cross correlation applied to unwrap - before and after.

However, in a more detailed inspection of the visual results, several noticeable faults (or interruptions of vertical continuity) can be seen where severe misplace occurs. These faults are caused by the settings of threshold in the module. Settings include the maximum drifting distance and maximum rotation error that can be compensated using the continuity property of camera record. If an obvious discontinuity of the texture of the surface occurs, it is not suitable for compensation, since visually it is impossible to tell if this discontinuity is caused by the camera vibration or it is just the natural appearance of geological de-

formation.

4.3 Camera Trajectory Smoothing

As a solution of the described problem above, a smoothing procedure with S-G filtered is tested to relatively reduce the incongruity of discontinuation. It recalculated the prediction values of Y using the algorithm in section 3.3. Here is the result before and after applying this smoothing method to unwrap the video in Figure 9. The red lines are the original trajectory drifting and rotation detected in the test of vibration compensation module. The blue lines represent the results after smoothing.

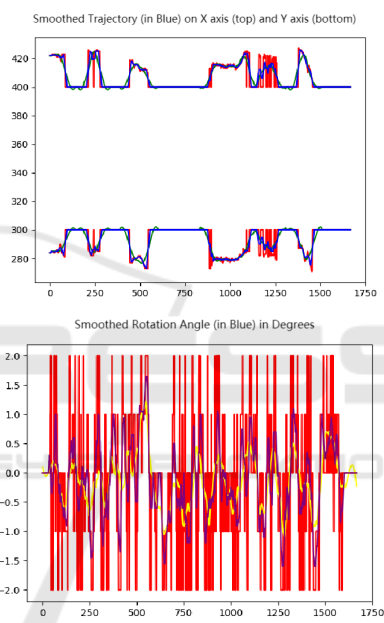


Figure 9: Smoothed trajectory of drift and rotation.

The performance is shown to be very effective, largely facilitating the problem of faults between rows and improving user experience when inspecting. It especially outperforms to smooth both rotation and drifting in a fast speed of calculation. In the Figure 10 of trajectory smoothing results below, a remarkable correction of errors can be seen in the block marked in red.

4.4 System Evaluation

Finally, the entire work flow of the designed system is implemented. Two testing boreholes are selected to examine the performance of the system. Here, the first test borehole is located in Deganwy, Wales[1].

In order to evaluate the performance quantitatively

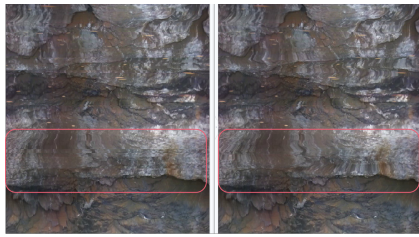


Figure 10: Smoothed results of unwrapping of the video.



Figure 11: Test results of borehole in Deganwy before(left) and after(right) processing.

to some extent, 18 locations of key points were manually labelled on the unwrapped image and a ground truth of inner surface generated by using ultra-sonic sensors and panoramic side view camera. The differences of according pixel locations between the output and ground truth are measured, thus the less the differences are, the better our borehole visualizer based on monocular camera works according to the results in Figure 12.

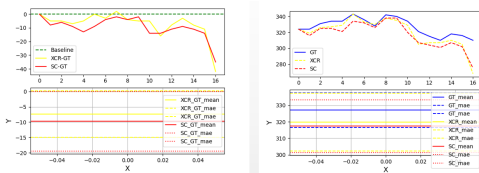


Figure 12: Quantitative results of trajectory comparing to ground truth.

For the ground truth, the camera trajectory is centralized in the borehole. Line in green is GT with no rotation error, and the yellow line represents the final output of the system. The average rotation error is measured at less than 8 pixels, which means 4 degrees. On the right, there are results of center position with values that represents the distance from center to the left edge of unwrapped image. Blue line represents the center of GT, and yellow line is the out-

put. The error of drifting in this figure stays within 10 pixels of distance, which is almost not noticeable for human eyes.

Results above proves that the system can produce good results, meaning that a simple monocular detector can be considered a powerful potential replacement of detectors with complicated sensors at higher price.

Here is another user test provided by sponsor company of the system (Figure 13):

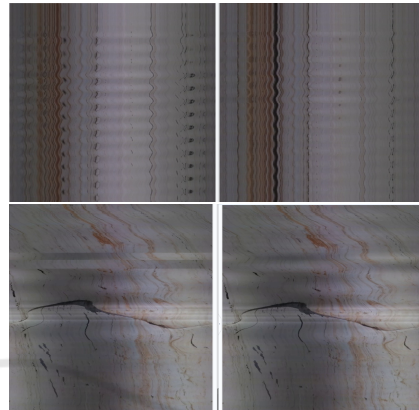


Figure 13: Test results of borehole in California.

As presented on the top two images of Figure 13, when a high-frequency circular swing of the detector is detected, results show that the unwrapped image is nicely compensated without interruptions and large distortions of the tracks of the textures on the inner surface. According to the feature of the designed system, this performance is expected and also proved to be able to handle high frequency vibrations, which are always encountered during utilization on-site.

5 CONCLUSIONS

This paper introduces a novel visualization approach for the inner surface of boreholes using only a monocular video camera. Three modules are designed to solve three related problems in logical order:

A Side-view unwrapping module was developed to sample the pixels on video frames and then project the coordinates of pixels from downwards view port to side view port, with the assumption of cylindrical shape in the normal case of artificially drilled boreholes. A distortion cancellation pre-processing stage is implemented first to cancel radial/tangential deformation of the image. Then a transfer of coordinates allows the extracted pixels to be remapped on side view, with configurable parameters of sampling position and unwrapping resolution.

A Vibration compensation module compensates the drift and rotation errors caused by friction, collisions and cable twist effects when lowering the detector into the borehole. Drift errors are fixed by finding the center position of boreholes on the video canvas with an ellipse finder that considers the dark 'bottom' area of the borehole as a potential center ellipse candidate of the cross-section of the borehole. Rotation errors are then compensated using cross-correlation which calculates the similarity and delay that can match two signals to the maximum. Two neighboring rows of extracted pixels are taken as input signals, and two threshold of similarity and delay are set to ensure the selected rows are suitable for compensation.

Finally, a camera trajectory smoothing module to handle the abrupt any changes of texture. In order to improve the visual presentation of the borehole inner surface, a Savitzky-Golay filter (S-G filter) is introduced to smooth the camera trajectory. Results show that the smoothing is effective as unexpected discontinuities brought about by vibration and data acquisition effects between rows are effectively eliminated.

To conclude, this system successfully accomplished a borehole inner surface visualization system with vibration cancellation and trajectory smoothing using only an optical monocular video camera. Results of experiments have demonstrated that the errors and interrupts are lowered to an unnoticeable level and the visualization performance is effectively improved.

Future improvements could include 3D reconstruction of boreholes based on simple monocular detector can be studied, involving Visual Simultaneous Localising and Mapping (V-SLAM) which is one of the most popular research topic in computer vision and reconstruction fields. This system is tested by commercial on-site utilization and it is believed to continue to perform robustly in future development of 2D to 3D modeling of boreholes as sophisticated visualiser and stabiliser of borehole inner surface inspection.

ACKNOWLEDGEMENTS

This research is supported by Robertson Geologging Ltd who provided access to equipment, software, expertise and commercial use cases to validate the accessibility and feasibility of the academic achievements as potential user products or services.

REFERENCES

- Al-Sit, W., Al-Nuaimy, W., Marelli, M., and Al-Ataby, A. (2015). Visual texture for automated characterisation of geological features in borehole televiewer imagery. *Journal of Applied Geophysics*, 119:139–146.
- Beauchemin, S. S. and Bajcsy, R. (2001). Modelling and removing radial and tangential distortions in spherical lenses. In Klette, R., Gimel'farb, G., and Huang, T., editors, *Multi-Image Analysis*, pages 1–21, Berlin, Heidelberg. Springer Berlin Heidelberg.
- Bereska, D., Daniec, K., Fraś, S., Jędrasiak, K., Malinowski, M., and Nawrat, A. (2013). System for multi-axial mechanical stabilization of digital camera. In *Vision Based Systems for UAV Applications*, pages 177–189. Springer.
- Cardani, B. (2006). Optical image stabilization for digital cameras. *IEEE Control Systems Magazine*, 26(2):21–22.
- Hartley, R. and Kang, S. B. (2007). Parameter-free radial distortion correction with center of distortion Estimation. *IEEE Transactions on Pattern Analysis and Machine Intelligence*, 29(8):1309–1321.
- Mur-Artal, R. and Tardós, J. D. (2017). Orb-slam2: An open-source slam system for monocular, stereo, and rgb-d cameras. *IEEE Transactions on Robotics*, 33(5):1255–1262.
- Pohl, C. and Genderen, J. L. V. (1998). Review article multisensor image fusion in remote sensing: Concepts, methods and applications. *International Journal of Remote Sensing*, 19(5):823–854.
- Press, W. H. and Teukolsky, S. A. (1990). Savitzky-golay smoothing filters. *Computers in Physics*, 4(6):669–672.
- Rajesh, R. J. and Kavitha, P. (2015). Camera gimbal stabilization using conventional pid controller and evolutionary algorithms. In *2015 International Conference on Computer, Communication and Control (IC4)*, pages 1–6.
- Souza, M. and Pedrini, H. (2019). Digital video stabilization: Algorithms and evaluation. In *Anais Estendidos do XXXII Conference on Graphics, Patterns and Images*, pages 35–41, Porto Alegre, RS, Brasil. SBC.
- Souza, M. R. and Pedrini, H. (2018). Digital video stabilization based on adaptive camera trajectory smoothing. *EURASIP Journal on Image and Video Processing*, 2018(1):1–11.
- Thiele, S. T., Lorenz, S., Kirsch, M., Cecilia Contreras Acosta, I., Tusa, L., Herrmann, E., Möckel, R., and Gloaguen, R. (2021). Multi-scale, multi-sensor data integration for automated 3-d geological mapping. *Ore Geology Reviews*, 136:104252.